Gas Sparged Adsorber for Decolourization Dye Effluent

Mamdouh M. Nassar[1], Taha E. Farrag[1] and Joseph Y. Farah[2]*

[1]Chemical Engineering Department, Faculty of Engineering, El-Minia University, El-Minia, Egypt

[2]Chemical Engineering & Pilot Plant Department, National Research Center, Dokki, Cairo, Egypt

Abstract

The adsorption of basic dyestuff (Maxilon Red BL-3) from aqueous solution at 25°C onto natural clay was studied. The clay showed high performance for dye removal, the maximum adsorption capacity of the natural clay was found to be 326 mg dye per g of natural clay. The experimental data were fitted to the Freundlich and Langmuir isotherm models. The best fitting isotherm was found to be the Langmuir isotherm. Mass balance calculation was carried out and the operating lines were used to calculate the amount of clay needed per unit volume of dye solution to reach the effluent concentration target. Gas sparged technique was proved to be very efficient technique, thus it was used to study the rate of dye removal from its solution using clay as adsorbent. A series of contact-time experiments was undertaken in a batch adsorber to assess the effect of the system variables, namely, gas flow rate, initial dye concentration, mass of clay and temperature of the solution, on the overall volumetric mass transfer coefficient. The study revealed that dye removal is diffusion controlled process.

Introduction

Multiphase flows are found in many applications of interest to industry. Bubble column reactors represent one broad class process equipment important to several industries in which multiphase flow phenomena are dominated. Examples include oxidation reactors used in the petrochemical industry, devices used in microbial fermentation and treatment of wastewater in biochemical industries [1] and environmental studies [2]. The widespread industrial applications of bubble column are due to its simple construction, large effective interfacial area and high mass transfer rates [1,3].

Adsorption techniques have proven successful in removing colored organics. Although activated carbon is very expensive and there is a need for regeneration after each adsorption cycle, it is the most widely used adsorbent because of its extended surface area, microporous structure, high adsorption capacity, and high degree of surface reactivity [4]. Consequently this cost problem has led to a search for cheap and efficient alternate materials [5].

Clay materials have been increasingly paid attention to because they are cheaper than activated carbons and have high specific surface area, chemical and mechanical stabilities. Also these have shown good results as an adsorbent for the removal of various metals, organic compounds and various dyes [6-8].

Little attention was given using gas sparged column as adsorber. Some experimental works are in progress for several years in our department [9-11]. In these studies, the dye removal from dye solutions was carried out using either gas stirring or mechanical stirring. The previous studies proved that gas stirring is more economic (higher removal rates in shorter time at lower energy consumption) than mechanical stirring. The high efficiency of gas sparging in increasing the rate of dye removal compared to single phase flow was attributed to the ability of gas bubbles to induce radial momentum transfer for the whole bulk, as well as to create turbulence behind the wake of each gas bubble [12].

The object of the present work is to study the equilibrium adsorption isotherm for basic dyes on natural clay to predict design data for batch system. The rates of mass transfer have been determined in order to investigate variables affecting adsorption process using gas sparging.

*corresponding author. E-mail: josephyfarah@hotmail.com

Printed in Kazakhstan

Materials and Methods

Natural clay was collected from El-Minia Governorate, Egypt. In previous work clay was found to be mainly montmorillonite type combined with about 10% Kaolinite [10], surface area of clay 65 m^2/g [13]. Clay was crushed, ground to a fine powder and sieved. Particle size used is in the range 500-700 μm and clay was used without any pre-treatment. Dyestuff was Basic Red 22 (Maxilon Red BL-3, Ciba Geigy) and its chemical structure is illustrated in Fig. 1. Concentration of dyestuff in aqueous solution was determined using a Spectra-Plus MKS spectrophotometer at a wavelength λ_{max} = 538 nm.

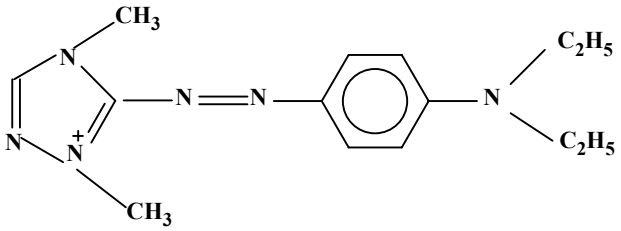

Fig. 1. Structure of the Maxilon Red BL-3.

Adsorption isotherm was determined by the bottle-point method [14]. A constant mass of clay (0.1 g) was added to bottles containing 50 ml of dye solution (different initial concentrations (50-500 ppm). The bottles were sealed and shaken at 700 rpm in a temperature-controlled shaker (25°C) until equilibrium was attained in 2 days.

Experimental set up for mass transfer study is shown in Fig. 2. The apparatus consisted mainly of vertical cylindrical jacketed glass column (60 cm height and 6 cm inside diameter). The column was fitted at its bottom with a G4 sintered-glass distributor with average diameter pores 5-10 microns. Next to gas distributor, a ball valve was fixed to control N_2 gas flow rate. Temperature was adjusted by passing hot water, thermostatically controlled, in the jacket around the column. Before each run, the column was filled with 1 liter of fresh dye solution at a certain concentration, followed by the addition of a known weight of clay after adjusting the gas-flow rate. The N_2 flow rate was measured with a calibrated rotameter. Samples were taken at 10 min. intervals. Several variables were studied, namely, gas flow rate, dye concentration, mass of clay and solution temperature.

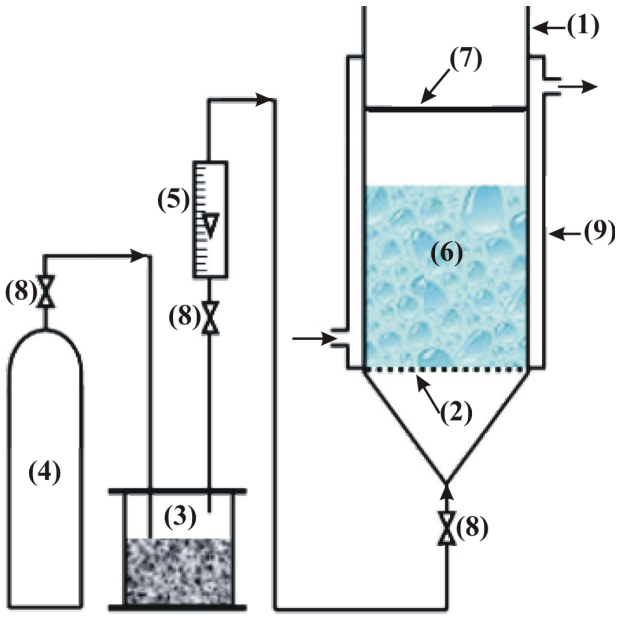

Fig. 2. Experimental apparatus: (1) Glass cylindrical column, (2) Sintered glass for gas distribution, (3) Gas humidifier, (4) Nitrogen cylinder, (5) Rotameter, (6) Fixed bed, (7) Solution level, (8) Control valves, (9) glass jacket.

Results and Discussion

Adsorption Isotherm

Adsorption isotherm of dye onto clay particles is shown in Fig. 3 as plot of q_e versus C_e. The data depicted in Figure 3 was further analyzed through the use of various adsorption isotherm equations. The Freundlich [15,16] and Langmuir [16,17] isotherm expressions are given by eqs. 1, 2 respectively:

$$q_e = K_f C_e^{\frac{1}{n}} \quad (1)$$

$$q_e = \frac{K_L C_e}{1 + a_L C_e} \quad (2)$$

where C_e is the equilibrium concentration (mg/l); q_e is the amount of dye sorbed at equilibrium (mg/g); K_f, n are the Freundlich isotherm constants and K_L, a_L are the Langmuir isotherm constants.

The obtained isotherm parameters are listed in Table 1. Results in Table 1, show that, the data obtained from the adsorption isotherm fitted to the Langmuir and Freundlich isotherm equations. Value of R_L is given in Table 1 and range between 0 and 1 indicating favorable adsorption [18] and the Freundlich exponent, n, is greater than unity, thereby indicating that the maxilon red dye is favorable adsorbed by clay [19].

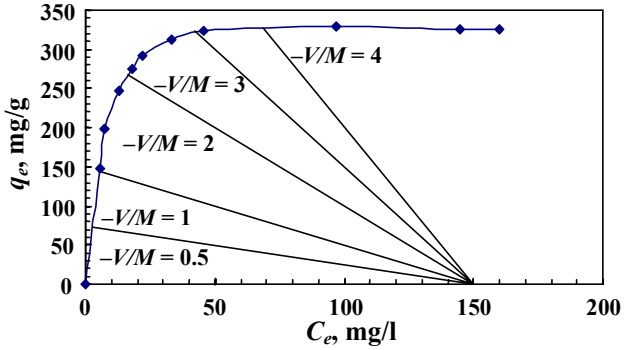

Fig. 3. Equilibrium adsorption isotherm for dye onto clay and operating lines with different slope values $-V/M$.

Table 1
Langmuir and Freundlich parameters

Langmuir parameters					Freundlich parameters		
K_L, l/g	a_L, l/mg	q_{max}^*, mg/g	R_L**	r***	K_f, l/g	n	r***
81.30	0.244	333.33	0.008	0.99	140.48	5.24	0.85

*Theoretical maximum adsorption capacity = K_L/a_L.
**Separation factor: $R_L = 1/(1 + aC_0)$, where C_0 is the maximum initial concentration.
***Correlation coefficient.

The empirical design procedures based on sorption equilibrium conditions are the most common methods to predict the adsorber size and performance. Previously, sorption isotherm relations have been used to predict the design of single stage batch adsorption systems [20].

The design objective is to reduce the dye solution of volume V (l) from an initial concentration of C_0 to C_1 (mg/l). The amount of adsorbent is M and the solute loading changes from q_0 to q_1 (mg/g). At time $t = 0$, $q_0 = 0$ and as time proceeds the mass balance equates the dye removed from the liquid to that picked up by the solid. A schematic diagram of a single stage batch adsorber is shown in Fig. 4. The mass balance equation for the sorption system in Fig. 4 can be expressed by equation 3.

$$VC_0 + Mq_0 = VC_1 + Mq_1 \qquad (3)$$

At the beginning, if fresh adsorbent is used, $q_0 =$ zero and at equilibrium conditions; $C_1 \rightarrow C_e$ and $q_1 \rightarrow q_e$ Rearranging eq. 3 gives:

$$\frac{M}{V} = \frac{C_0 - C_e}{q_e} \qquad (4)$$

or

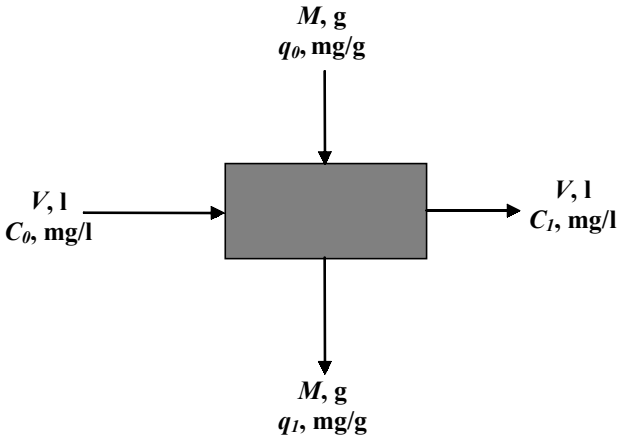

Fig. 4. Single stage batch adsorber design.

$$q_e = \frac{-V}{M}C_e + \frac{V}{M}C_0 \qquad (5)$$

The material balance provides the operating line equation in Fig. 3. The equilibrium sorption capacity q_e for any initial dye concentration can be obtained from the operating line and the isotherm Fig. 3. Where $-V/M$ is the slope of the operating lines; q_e, C_e can be found from Fig. 3 and thus mass of clay per unit volume of dye solution can be evaluated to reach C_e (target effluent concentration).

Figure 3 shows series of operating lines with different slopes (ratios of dye solutions to masses of clay) at 150 mg/l initial dyes concentrations. The predicted q_e, C_e values for different initial dye concentrations at different V/M ratios are shown in Table 2.

Table 2
Calculation of the sorption capacity and percent dye removal at 150 mg/l initial dye concentration and different values of V/M

V/M, l/g	Equilibrium Dye Concentration, mg/l	Adsorption Capacity, mg/g	Removal, %
4	68.5	326	54.3
3	42.5	322.5	71.7
2	16.4	267.2	89.1
1	5.5	144.5	96.3
0.5	3	73.5	98.0

Rate of Adsorption

Rate of dye removal was followed by conducting a series of contact time for the adsorption of dye on

clay by varying different operating parameters. Figure 5 shows a typical contact-time study. The curves represent concentration-time profiles for clay-dyes adsorption system using gas stirring. There is a high rate of colour removal between 20 and 60 min, followed by a plateau (constant rate) when equilibrium stage is reached. Increasing gas flow rate lead to decrease in the resistance of the boundary film surrounding the clay particles and increase the diffusion of dyes until the clay particles are saturated and equilibrium state is reached after about one hour.

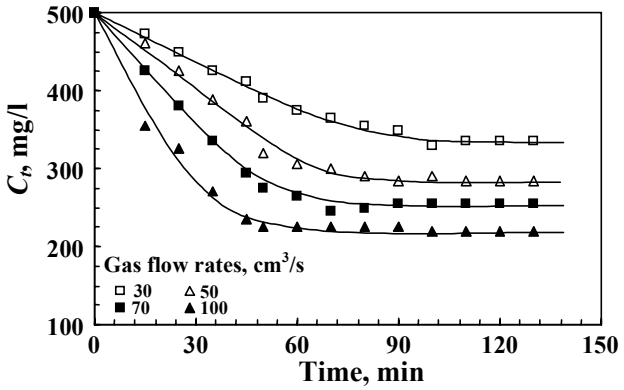

Fig. 5. Effect of gas sparging on the rate of colour removal (C_0 = 500 mg/l, M = 2 g, t = 25±1°C).

The overall process of adsorption of dyes on clay can be simulated by equation 6:

$$-V\frac{dC}{dt} = kAC \qquad (6)$$

where the overall mass transfer coefficient k can be defined by equation 7:

$$\frac{1}{k} = \frac{1}{k_1} + \frac{1}{k_2} \qquad (7)$$

where k_1 is the external mass transfer coefficient and k_2 is the mass transfer coefficient due to intraparticle diffusion (cm/s).

Integrating, equation 6, yields,

$$\ln(C_0 / C_t) = \frac{kAt}{V} = Kt \qquad (8)$$

where K is the overall volumetric mass transfer coefficient (cm/s), which can be obtained from the plots of $\ln(C_0/C)$ versus time at different parameters.

Effect of Gas Flow Rate

Figures 5, 6 shows the effect of nitrogen flow rate on the rate of adsorption. It is observed that increasing gas flow rate leads to decrease in the resistance of the boundary film surrounding the clay particles and increase the diffusion of dyes until the clay particles are saturated and equilibrium state is reached after about one hour. These results can be represented by Figure 7 from which illustrates a linear relation between ln$Q$ and ln$K$, where Q is gas flow rate and K represents the over all mass transfer coefficient. The increase of mass transfer by increasing gas flow rate is attributed to the ability of rising bubble swarm to include axial turbulent flow as well as radial flow. Turbulence results in decreasing the diffusion layer thickness at the clay surface with a consequently increase in the mass transfer coefficient [10]. The data given in Fig. 7 fit the equation:

$$K = (9.69\times10^{-5})Q^{1.145} \qquad (9)$$

Effect of Initial Concentration

A given mass of clay can only adsorb a certain amount of dye. Therefore, the higher the concentra-

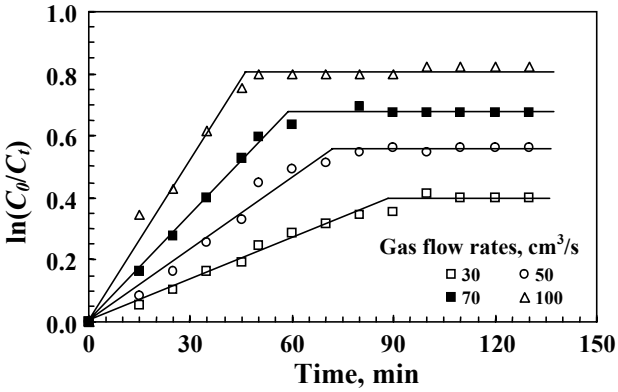

Fig. 6. ln(C_0/C_t) versus time for different gas flow rates (C_0 = 500 mg/l, M = 2 g, t = 25±1°C).

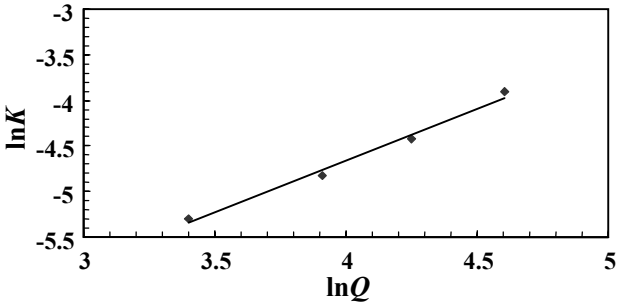

Fig.7. Relation between ln$Q$ (gas flow rate) and ln$K$ (overall mass transfer coefficient).

tion of the dye in the solution, the smaller the volume of solution that a fixed mass of clay can purify. The mass transfer coefficient was found to decrease with the increase of initial dye concentration as shown in Fig. 8 and these results are in agreement with previous result in the literature [21]. The low mass transfer rate at high concentration compared to the high mass transfer rate at low concentration can be explained on the basis that the gathering of dye molecules due to collision can reduce the activity coefficient of the dye and its effective diffusivity. The calculated values of the overall volumetric mass transfer coefficient can be plotted against the initial concentrations as shown in Fig. 9. The results were found to fit the following equation:

$$K = 15.919C_0^{-1.187} \quad (10)$$

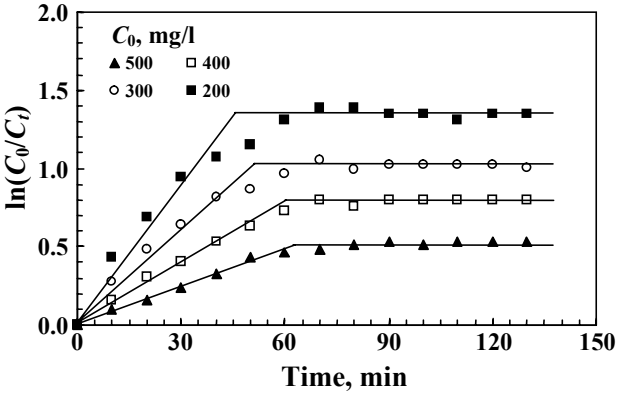

Fig. 8. $\ln(C_0/C_t)$ versus time for different initial concentrations (Q = 50 cm^3/s, M = 2 g, t = 25±1°C).

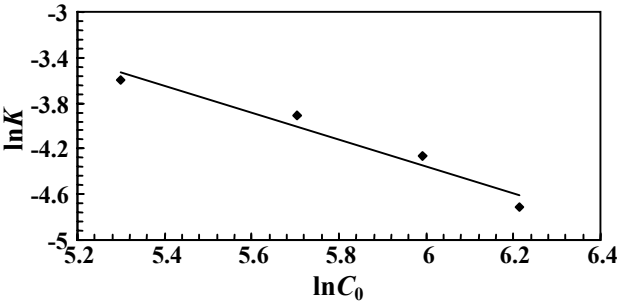

Fig. 9. Relation between lnC_0 (initial dye concentration) and ln$K$ (overall mass transfer coefficient).

Effect of Clay Mass

Figure 10 shows the effect of clay mass on the mass transfer coefficient. In general, mass transfer coefficient depends on driving force per unit area. Therefore, increasing mass of clay leads to increase the available surface area which explains the increase of mass transfer coefficient with increasing mass of clay. The mass transfer coefficients were determined and they are represented versus mass of clay as shown in Fig. 11. A linear relationship was obtained; the data in Fig. 11 fit the equation:

$$K = (4.514\times10^{-3})m^{1.225} \quad (11)$$

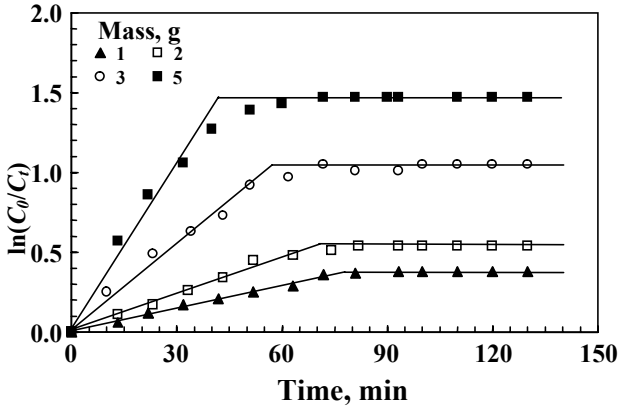

Fig. 10. $\ln(C_0/C_t)$ versus time for different masses of clay, (Q = 500 cm^3/s, C_0 = 500 mg/l, t = 25±1°C).

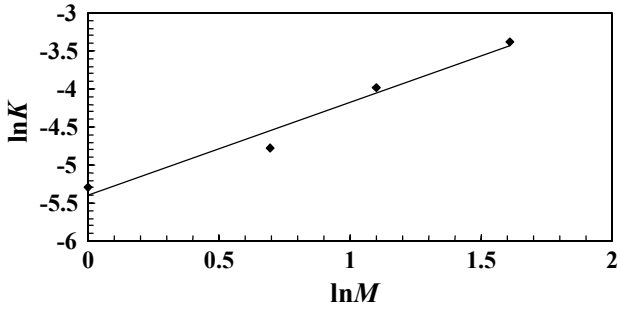

Fig. 11. Relation between ln$M$ (mass of clay) and ln$K$ (overall mass transfer coefficient).

Effect of Temperature

Figure 12 shows the effect of temperature on the mass transfer coefficient. The coefficient increased with increasing the temperature of the solution. This may be attributed to the decrease of the viscosity of the dye solution with the temperature. The mass transfer coefficient tends to increase with decreasing solution viscosity, probably because of the increase of dye ion diffusivity owing to the decrease in the diffusion layer thickness at the surface of the clay particles according to the relation.

$$K = D/\delta \quad (12)$$

where K is the mass transfer coefficient, D is the diffusivity, δ is the boundary layer thickness.

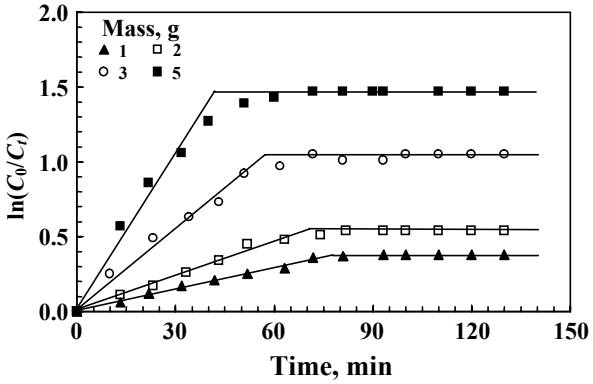

Fig. 12. $\ln(C_0/C_t)$ versus time for different temperatures (Q = 50 cm^3/s, C_0 = 500 mg/l, M = 2 g).

Figure 13 depict the relation of the mass transfer coefficients obtained from Fig. 12 versus temperatures. The data given in Figure 13 fit the following equation:

$$K = (2.355\times10^{-4})T^{1.08} \qquad (13)$$

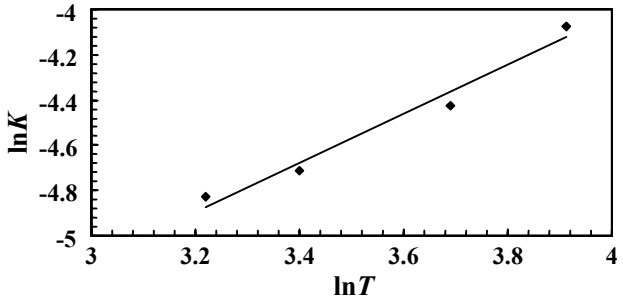

Fig. 13. Relation between ln$T$ (temperature of the mixture) and ln$K$ (overall mass transfer coefficient).

Conclusions

The present study shows that natural clay can be effectively used as an adsorbent for the removal of Maxilon Red BL-3 from its aqueous solution. The equilibrium data were found to be well represented by the Freundlich and Langmuir. Operating lines from material balance calculations can be used in the design of single stage batch adsorber for different liquid/ solid ratio (V/M) using the experimental equilibrium data.

The high efficiency of gas sparging adsorber in removal of dye solution onto clay was attributed to the ability of gas bubbles to induce radial and axial momentum transfer inside the whole bulk solution. Diffusion of dyes occurred from bulk of solution to the clay surfaces. The surface area of clay was 65 m^2/g. The adsorption of dyes on clay particles was irreversible process.

References

1. Padial, T., Vander-Heyden, W.B., Rauenzalen, R.M., and Yarbo, S.L., Chem. Eng. Sci. 55:3261 (2000).
2. Jia, Y., Wang, R., and Fane, A.G., Chem. Eng. J. 116:53 (2006).
3. Shaaban, N.A., Chem. Eng.&Technol. 26:1151 (2003).
4. Lin,S., Juangb, R., and Wanga, Y., J. Hazard. Mater. B 113:195 (2004).
5. Özcan,A., Erdem, B., and Özcan, A., J. Colloid. Interface. Sci. 280:44 (2004).
6. Unuabonah, E.I., Olu-Owolabi, B.I., Adebowale, K.O., and Ofomaja, A.E., Colloid Surf. A: Physicochem. Eng. Asp. 292:202 (2007).
7. Qiuhong, H., Zhiping, X., Shizhang, Q., Haghseresht, F., Wilson, M., and Lu, G.Q., J. Colloid. Interface. Sci. 308:191 (2007).
8. Huang, J., Liu, Y., Qingzhe, J., Wang, X., and Yang, J., J. Hazard. Mater. 143:541 (2007).
9. Nassar, M. Mamdouh. Wat. Res. 32:3071 (1998).
10. Nassar, M.M., and Yehia, H.M., Indian Chem. Eng. 41:27 (1999).
11. Nassar, M.M., Fadali, O.A., and Reda, A.A., Gas stirring technique for adsorption of dyes onto montmorillonite clay. Sustainable Energy and Environmental Technology-Asian Pacific Conf., Ed. Hu and Yue, World Publisher, Hong Kong, 2001, p. 479.
12. Kast, W., Intern J. Heat Mass Transf. 5:329 (1962).
13. Farah, J.Y., "Uses clay in removal of nickel from waste water" MSc Thesis El-Minia Uni. Egypt. 1992.
14. El-Geundi, M., Adsorp. Sci. Technol. 7:114 (1990).
15. Freundlich, H. M. F., Zeitschrift für Physikalische Chemie 57: 385 (1906).
16. Karnitz, O., Guregel, L.V.A., Melo, J.C.P., Botaro, V.R., Melo, T.M.S., Freitas Gil, R.P.F., Frederic,L., Bioresour. Technol. 98:1291(2007).
17. Langmuir, I., J. of the American Chem. Society 38:2221 (1916).
18. Weber, T.W., and Chakravorti, R.K., AIChE. J. 20:223 (1974).
19. Treybal, R.E. Mass Transfer Operations. 3-rd Edn, Mc Graw-Hill, New York 1980.
20. Kumar, K.V., and Porkodi, K., Dyes and pigment 74:590 (2007).
21. McKay, G.; and Allen, S.J. Canad. J. Chem. Eng. 58:521 (1983).

Received 13 February 2007.